An anaerobic mitochondrion that produces hydrogen

Boxma, Brigitte; Graaf, Rob M. de; Staay, Georg W.M. van der; Alen, Theo A. van; Ricard, Guenola; Gabaldón, Toni; Hoek, Angela H.A.M. van; Moon-van der Staay, Seung Yeo; Koopman, Werner J.H.; Hellemond, Jaap J. van

Published in:
Nature

DOI:
10.1038/nature03343

Publication date:
2005

subject to the constraints that no lichen covered the trunk and no young trees with a trunk circumference less than 0.9 m were used. Colour matches of treatments to natural bark were verified by spectrophotometry of stimuli and bark, followed by modelling of predicted photon catches[16] of a typical passerine bird, the blue tit's (*Parus caeruleus*) single cone photoreceptors[17], with irradiance spectra from overcast skies in the study site. Our acceptance criterion was simply that cone captures for the experimental stimuli fell within the measured range of those for oak bark.

Experiment 1 used black patterns printed onto dark brown card. Patterns were samples of digital photos of the oak trees at 1:1 reproduction, converted using ImageJ[18] to greyscale and thresholded at 50% to binary (black/white) images to provide, when printed onto brown card, bark-like brown/black spatial variation (Fig. 1). Different samples, from different trees, were used for each replicate target.

Experiment 2 used bicoloured targets printed onto waterproof paper (Hewlett Packard Laserjet Tough Paper) with a Hewlett Packard Colour Laserjet 2500 (600 dots per inch) printer, with colour pairs chosen to have either high or low contrast. Colours were chosen from frequency distributions of the eight-bit RGB (red, green, blue) values from digital photographs of the oak trees in the study site, reduced to 16 bins in each colour channel. Photos (about 267 mm × 200 mm; 2,560 pixels × 1,920 pixels) were taken with a Nikon Coolpix 5700 camera, calibrated[19] to linearize the relationship between radiance and the greyscale in each colour channel, and saved as uncompressed TIFF files. Digital photographs lack ultraviolet information that birds can see[20], but lichen-free oak bark reflects negligible ultraviolet[21]. Even a properly calibrated RGB image does not precisely simulate the avian-perceived colour of many natural objects, owing to differences in the spectral sensitivity of bird long-wave, medium-wave and short-wave cones compared with human cones[22]. However, because our treatments varied only in relative colour contrast, any error associated with this method was considered minor, an assumption verified retrospectively by spectrophotometry and colour-space modelling. We chose colour pairs from the eight most frequent RGB triplets in the bark photos as follows: a 'background' colour, then a triplet that was similar to the background (low contrast), and one that differed markedly (high contrast). The major difference between colours was in overall brightness not hue, but we could not systematically vary only one colour dimension within the available common bark colours. Sample numbers of background and contrasting colours were balanced for which was darker/lighter, and so there were no significant differences between bicoloured treatments in the brightest or darkest colour or average colour (analyses of variance on RGB sums and all possible ratios; $P > 0.9$). Monochrome treatments were also created as the means of the respective R, G and B values of the two colours in bicoloured high-contrast and low-contrast treatments. Different colour pairs and patterns, from different trees, were used for each replicate target.

Survival analysis was by Cox regression[23,24] with the factors treatment and block. Cox regression assumes that all survival functions have the same shape; this proportional hazards assumption was checked by plotting partial residuals against ranked survival times[24]. There were significant block effects in both experiments (in experiment 1, Wald = 121.78, d.f. = 9, $P < 0.001$; in experiment 2, Wald = 271.50, d.f. = 9, $P < 0.001$), reflecting differences in average predation rates in different parts of the woods on different dates, but this was not relevant to our hypotheses.

Received 23 September; accepted 30 December 2004; doi:10.1038/nature03312.

1. Endler, J. A. Progressive background in moths, and a quantitative measure of crypsis. *Biol. J. Linn. Soc.* **22,** 187–231 (1984).
2. Endler, J. A. An overview of the relationships between mimicry and crypsis. *Biol. J. Linn. Soc.* **16,** 25–31 (1981).
3. Thayer, G. H. *Concealing Coloration in the Animal Kingdom; An Exposition of the Laws of Disguise through Color and Pattern; Being a Summary of Abbott H. Thayer's Discoveries* (Macmillan, New York, 1909).
4. Cott, H. B. *Adaptive Coloration in Animals* (Methuen, London, 1940).
5. Merilaita, S. Crypsis through disruptive coloration in an isopod. *Proc. R. Soc. Lond. B* **265,** 1059–1064 (1998).
6. Silberglied, R. E., Aiello, A. & Windsor, D. M. Disruptive coloration in butterflies - lack of support in *Anartia fatima*. *Science* **209,** 617–619 (1980).
7. Behrens, R. R. *False Colors: Art, Design and Modern Camouflage* (Bobolink, Dysart, Iowa, 2002).
8. Thayer, A. H. The law which underlies protective coloration. *Auk* **13,** 124–129 (1896).
9. Endler, J. A. On the measurement and classification of colour in studies of animal colour patterns. *Biol. J. Linn. Soc.* **41,** 315–352 (1990).
10. Endler, J. A. A predator's view of animal color patterns. *Evol. Biol.* **11,** 319–364 (1978).
11. Bennett, A. T. D., Cuthill, I. C. & Norris, K. J. Sexual selection and the mismeasure of color. *Am. Nat.* **144,** 848–860 (1994).
12. Kiltie, R. A. Countershading: universally deceptive or deceptively universal? *Trends Ecol. Evol.* **3,** 21–23 (1988).
13. Ruxton, G. D., Speed, M. P. & Kelly, D. J. What, if anything, is the adaptive function of countershading? *Anim. Behav.* **68,** 445–451 (2004).
14. Waldbauer, G. P. & Sternburg, J. G. A pitfall in using painted insects in studies of protective coloration. *Evolution* **37,** 1085–1086 (1983).
15. Merilaita, S., Tuomi, J. & Jormalainen, V. Optimization of cryptic coloration in heterogeneous habitats. *Biol. J. Linn. Soc.* **67,** 151–161 (1999).
16. Maddocks, S. A., Church, S. C. & Cuthill, I. C. The effects of the light environment on prey choice by zebra finches. *J. Exp. Biol.* **204,** 2509–2515 (2001).
17. Hart, N. S., Partridge, J. C., Cuthill, I. C. & Bennett, A. T. D. Visual pigments, oil droplets, ocular media and cone photoreceptor distribution in two species of passerine: the blue tit (*Parus caeruleus* L.) and the blackbird (*Turdus merula* L.). *J. Comp. Physiol. [A]* **186,** 375–387 (2000).
18. Rasband, W. *ImageJ* v. 1.30 (http://rsb.info.nih.gov/ij/docs/, National Institutes of Health, USA, 2003).
19. Parraga, C. A., Troscianko, T. & Tolhurst, D. J. Spatiochromatic properties of natural images and human vision. *Curr. Biol.* **12,** 483–487 (2002).
20. Cuthill, I. C. *et al.* Ultraviolet vision in birds. *Adv. Stud. Behav.* **29,** 159–214 (2000).
21. Majerus, M. E. N., Brunton, C. F. A. & Stalker, J. A bird's eye view of the peppered moth. *J. Evol. Biol.* **13,** 155–159 (2000).
22. Cuthill, I. C. *et al.* Avian colour vision and avian video playback experiments. *Acta Ethol.* **3,** 29–37 (2000).
23. Cox, D. R. Regression models and life-tables. *J. R. Stat. Soc. B* **34,** 187–220 (1972).
24. *SPSS for Windows Release 9.0* (SPSS Inc., Chicago, 2003).

Acknowledgements We thank J. Endler for suggestions. The research was supported by a BBSRC grant to I.C.C., T.S.T. and J. C. Partridge.

Authors' contributions I.C.C. designed the experiments and stimuli; M.S., J.S., T.M. and I.C.C. performed the experiments; A.P. wrote the programs for colour analysis and camera calibration; T.S.T. advised on design and colour modelling.

Competing interests statement The authors declare that they have no competing financial interests.

Correspondence and requests for materials should be addressed to I.C. (i.cuthill@bristol.ac.uk).

An anaerobic mitochondrion that produces hydrogen

Brigitte Boxma[1]*, Rob M. de Graaf[1]*, Georg W. M. van der Staay[1]*, Theo A. van Alen[1], Guenola Ricard[2], Toni Gabaldón[2], Angela H. A. M. van Hoek[1]†, Seung Yeo Moon-van der Staay[1], Werner J. H. Koopman[3], Jaap J. van Hellemond[4], Aloysius G. M. Tielens[4], Thorsten Friedrich[5], Marten Veenhuis[6], Martijn A. Huynen[2] & Johannes H. P. Hackstein[1]

[1]*Department of Evolutionary Microbiology, Faculty of Science, Radboud University Nijmegen, Toernooiveld 1, NL-6525 ED Nijmegen, The Netherlands*
[2]*Centre for Molecular and Biomolecular Informatics,*
[3]*Microscopical Imaging Centre and Department of Biochemistry, Nijmegen Centre of Molecular Life Sciences (NCMLS), Radboud University Nijmegen Medical Centre, NL-6500 HB Nijmegen, The Netherlands*
[4]*Department of Biochemistry and Cell Biology, Faculty of Veterinary Medicine, Utrecht University, PO Box 80176, NL-3508 TD Utrecht, The Netherlands*
[5]*Albert-Ludwigs-Universität, Institut für Organische Chemie und Biochemie, Albertstrasse 21, D-79104 Freiburg i. Br., Germany*
[6]*Department of Eukaryotic Microbiology, Groningen University, PO Box 14, NL-9750 AA Haren, The Netherlands*

* These authors contributed equally to this work
† Present address: RIKILT, Institute of Food Safety, Bornsesteeg 45, NL-6708 PD Wageningen, The Netherlands

Hydrogenosomes are organelles that produce ATP and hydrogen[1], and are found in various unrelated eukaryotes, such as anaerobic flagellates, chytridiomycete fungi and ciliates[2]. Although all of these organelles generate hydrogen, the hydrogenosomes from these organisms are structurally and metabolically quite different, just like mitochondria where large differences also exist[3]. These differences have led to a continuing debate about the evolutionary origin of hydrogenosomes[4,5]. Here we show that the hydrogenosomes of the anaerobic ciliate *Nyctotherus ovalis*, which thrives in the hindgut of cockroaches, have retained a rudimentary genome encoding components of a mitochondrial electron transport chain. Phylogenetic analyses reveal that those proteins cluster with their homologues from aerobic ciliates. In addition, several nucleus-encoded components of the mitochondrial proteome, such as pyruvate dehydrogenase and complex II, were identified. The *N. ovalis* hydrogenosome is sensitive to inhibitors of mitochondrial complex I and produces succinate as a major metabolic end product—biochemical traits typical of anaerobic mitochondria[3]. The production of hydrogen, together with the presence of a genome encoding respiratory chain components, and biochemical

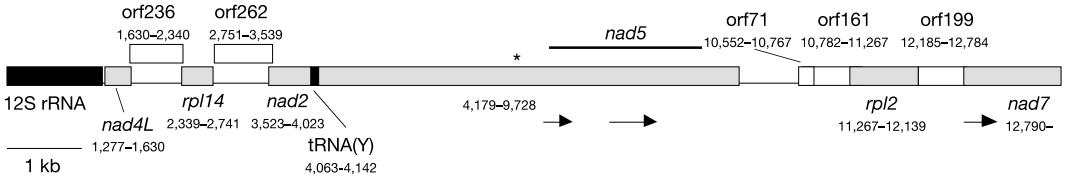

Figure 1 A 14,027-bp fragment (mtg 1) of the hydrogenosomal genome of *N. ovalis* var. *Blaberus* Amsterdam. Black boxes, RNA coding genes; shaded boxes, genes with significant similarity to mitochondrial genes; white boxes, unknown ORFs (named according to the number of codons); arrows, cDNAs identified so far. The numbers indicate the nucleotide positions on the 14-kb clone (mtg 1). The longest ORF (4,179–9,728) contains a stretch with significant similarity to *nad5*. A potential start codon for a putative *nad5* transcript is marked with an asterisk.

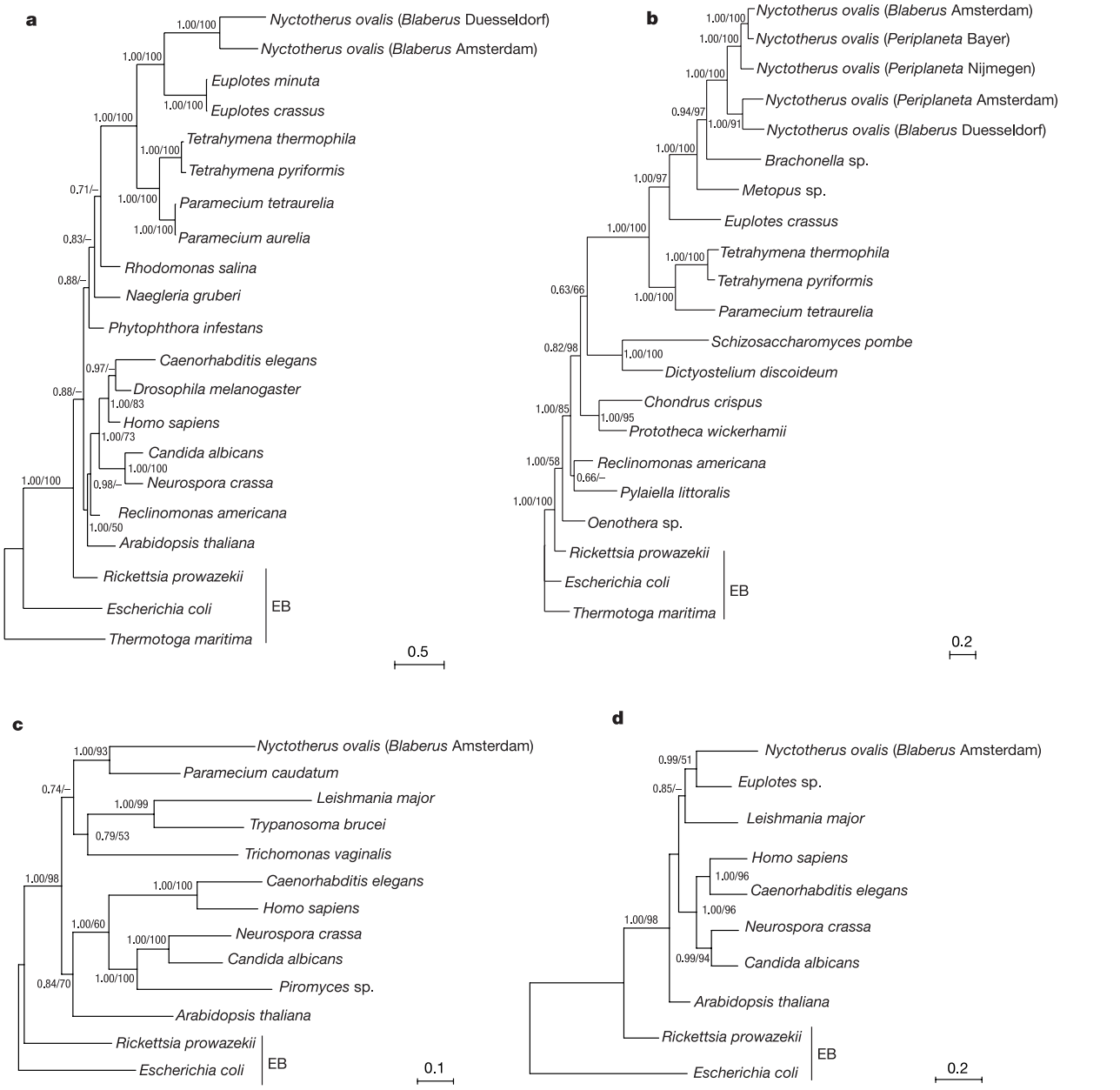

Figure 2 Phylogenetic analysis of hydrogenosomal genes. Both the organellar 12S (SSU) rRNA gene (**b**) and the nuclear hsp60 (**c**) reveal a ciliate ancestry for the hydrogenosome of *N. ovalis*. The same is true for the components of a 'mitochondrial' complex I, the *nad7* (49 kDa; organellar, **a**) and *51 kDa* (nuclear, **d**) genes. The phylogenies were derived using MrBayes and neighbour joining: the topologies correspond to the maximum-likelihood (MrBayes) approach, and the values at the nodes indicate the posterior probability for the partition and its bootstrap value, respectively. Only values higher than 50% are indicated. See Supplementary Information. EB, Eubacteria.

features characteristic of anaerobic mitochondria, identify the *N. ovalis* organelle as a missing link between mitochondria and hydrogenosomes.

Hydrogenosomes and their highly reduced relatives, mitosomes, generally lack an organelle genome[5–8], hampering clarification of their origin. Two models for the origin of hydrogenosomes are currently debated. The first posits that the ancestral mitochondrial endosymbiont gave rise to aerobically functioning mitochondria, which subsequently evolved into hydrogenosomes by the acquisition of genes encoding enzymes essential for an anaerobic metabolism[9–13]. The second hypothesis presumes that hydrogenosomes and mitochondria originated from one and the same ancestral—facultatively anaerobic—(endo)symbiont, followed by specialization to aerobic and anaerobic niches during eukaryotic evolution[13,14].

To address this issue we investigated DNA in hydrogenosomes of *N. ovalis*, which was previously identified by immunocytochemical methods[15]. Intact *N. ovalis* hydrogenosomes isolated by cell fractionation contained DNA between 20 and 40 kilobases (kb) long. Long-range polymerase chain reaction (PCR) with this DNA with the use of specific primers for the hydrogenosomal small-subunit (SSU) ribosomal RNA[15] and *nad7* (obtained earlier by PCR with degenerated primers) yielded a 12-kb fragment of the organellar genome. It encodes four genes of a mitochondrial complex I (*nad2*, *nad4L*, *nad5* and *nad7*), two genes encoding mitochondrial ribosomal proteins RPL 2 and RPL 14, and a ^{tyr}tRNA gene (Fig. 1). *Nad2* and *nad4L*, which are generally poorly conserved among ciliates, could be identified by using multiple sequence alignments and an analysis of their membrane-spanning domains as described

Table 1 ***Nyctotherus ovalis* genes encoding mitochondrial proteins and RNAs**

Type	Gene product	Localization of the gene	Codon use	cDNA	Target signal	Accession no.
Mt complex I	NAD2	H	Mt		No	AJ871267
	NAD4L	H	Mt		No	AJ871267
	NAD5	H	Mt	Yes*	No	AJ871267
	NAD7	H	Mt	Yes†	No	AJ871267
	24 kDa	N	Nuc		Yes	AY628688
	51 kDa	N	Nuc	Yes‡	Yes	AY608632
	75 kDa	N	Nuc		Yes	AJ871573
Mt complex II	SDH a	N	Nuc	Yes§	Yes	AY616152
	SDH b	N	Nuc	Yes‖	Yes	AY619980
Mt protein synthesis	Putative rRNA methyltransferase 2	N	Nuc			AJ871313
Mt ribosomal proteins	RPL 2	H	Mt			AJ871267
	RPL 14	H	Mt			AJ871267
	RPL 20	N	Nuc		?	AJ871314
Mt tRNA	tRNA tyrosine	H	rna			AJ871267
Mt rRNA	12S rRNA (SSU)	H	rna			AJ871267
Mt catabolism/energy metabolism	PDH E1α	N	Nuc	Yes¶	Yes	AY623917
	PDH E1β	N	Nuc	Yes**	Yes	AY628683
	PDH E2	N	Nuc	Yes††	Yes	AY623925
	[Fe] Hydrogenase	N	Nuc	Yes‡‡	Yes	AY608627
	Acetyl-coenzyme A synthase 2 (EC 6.2.1.1)	N	Nuc		No	AJ871315
	Adenylate kinase 2 (EC 2.7.4.3)	N	Nuc		No	AJ871316
	Adenylate kinase 2 isoform c = HK2418	N	Nuc			AJ871317
	Probable D-lactate dehydrogenase [cytochrome] (EC 1.1.2.4)	N	Nuc		Yes	AJ871318
	Succinyl-CoA ligase	N	Nuc		Yes	AJ871319
	Succinyl-CoA:3-ketoacid-coenzyme A transferase	N	Nuc		Yes	AJ871320
	Glycerol kinase	N	Nuc		?	AJ871321
Mt carrier family	AAC	N	Nuc		No	AF480921
	Putative mt carrier protein PET8 YNL003C_Chr	N	Nuc		No	AJ871322
Mt import/processing	Mt processing peptidase alpha subunit	N	Nuc		?	AJ871323
	HSP 60	N	Nuc		Yes	AJ871324
	HSP 70	N	Nuc		No	AJ871325
	Heat shock protein HSP82 YMR186W_Chr	N	Nuc		No	AJ871326
	TOM 34	N	Nuc		No	AJ871327
	Mt protein import protein MAS5 (Protein YDJ1)	N	Nuc		?	AJ871328
	Stress-70 protein, mt precursor	N	Nuc		?	AJ871329

For a complete table see Supplementary Information. N, nucleus; H, hydrogenosome; nuc, nuclear; mt, mitochondrial; mtg 1, 12-kb clone of hydrogenosomal genome (AJ871267); ?, low-probability support so far because full-length cDNAs have not yet been isolated (the N terminus might be incomplete, or it might contain an in-frame intron or alternative start codons).
Accession numbers for cDNAs: * AJ871574 and AJ871575; † AJ871576; ‡AY608633 and AY608634; §AY616150 and AY616151; ‖AY619981; ¶AY623919; **AY628684; ††AY623926; ‡‡AY608633 and AY608634.

Table 2 **Glucose metabolism of *Nyctotherus ovalis***

Labelled end products	[U-^{14}C]glucose		[6-^{14}C]glucose	
	(μmol h^{-1} per mg protein)	(%)*	(μmol h^{-1} per mg protein)	(%)*
Acetate	427	53	467 ± 87	65 ± 22
Lactate	220	27	156 ± 116	20 ± 13
Succinate	112	14	79 ± 65	10 ± 7
Ethanol	44	5	29 ± 26	4 ± 3
CO_2	205	–	ND	–
Formate	ND	–	ND	–

Cells were incubated for 48 h at 25 °C in micro-aerobic conditions in medium with either [U-^{14}C]glucose or [6-^{14}C]glucose. Excreted end products are shown as means ± s.d. of three independent experiments ([6-^{14}C]glucose) or as the means of two independent experiments ([U-^{14}C]glucose). Other excreted end products were less than 2% of the total excreted end products. ND, not detectable.
*Percentage of the total of acetate, lactate, succinate and ethanol.

previously[16]. Phylogenetic analysis revealed clustering of these genes with their homologues from the mitochondrial genomes of aerobic ciliates (Fig. 2, and Supplementary Information). All genes exhibit a characteristic mitochondrial codon-usage and lack amino-terminal extensions that could function as a mitochondrial targeting signal (Table 1). Complementary DNAs isolated for *nad5* and *nad7* show that they are transcribed. Translation with a nuclear genetic code from *N. ovalis*, rather than the ciliate mitochondrial code, leads to numerous stop codons (not shown). Five additional open reading frames (ORFs 236, 262, 71, 161 and 199) do not show significant sequence similarity to ORFs from the mitochondrial genomes accessible in the EMBL database. Two ORFs overlap with neighbouring ORFs as in other mitochondrial genomes[17].

Macronuclear gene-sized chromosomes encoding the 24-kDa, 51-kDa and 75-kDa subunits of mitochondrial complex I and the Fp and Ip subunits of mitochondrial complex II were cloned with a PCR-based approach. These have a nuclear codon usage, are transcribed (Table 1), encode a putative N-terminal mitochondrial targeting signal and branch with their mitochondrial homologues from aerobic ciliates in phylogenetic analyses (Fig. 2, Table 1 and Supplementary Information). They are similar to the two complex I-like Ndh51 and Ndh24 proteins discovered in *Trichomonas vaginalis*[18,19], because a phylogenetic analysis including the mitochondrial homologues from *N. ovalis* and certain aerobic ciliates reveals that all these proteins belong to a cluster of mitochondrial complex I homologues (see Supplementary Information). Thus, in *N. ovalis*, 7 of the 14 genes encoding core proteins of mitochondrial complex I, and two of the four proteins of mitochondrial complex II, have been identified so far. They are well conserved, are transcribed, and cluster with the mitochondrial homologues of their aerobic (ciliate) relatives, indicating that the hydrogenosomes of *N. ovalis* have retained parts of a functional mitochondrial electron-transport chain.

Hydrogenosomes of *N. ovalis* have typical mitochondrial cristae and contain cardiolipin[11]. They are closely associated with endosymbiotic methanogens, which are biomarkers for hydrogen formation by the *N. ovalis* hydrogenosomes[20] (Fig. 3a). The organelles stain with Mitotracker Green FM and fluoresce with rhodamine 123, indicating the presence of a membrane potential (Fig. 3). Carbonyl cyanide *p*-trifluoromethoxyphenylhydrazone (FCCP) (5 μM) prevented staining with rhodamine 123, indicating the possible presence of a proton gradient. Moreover, staining of the hydrogenosomes with rhodamine 123 was also prevented after incubation of the ciliates with rotenone, piericidin, fenazaquin and 1-methyl-4-phenylpyridinium (MPP^+) (classical inhibitors of mitochondrial complex I (ref. 21)), but not with cyanide (1 mM) or antimycin A (inhibitors of mitochondrial complex III and IV; Fig. 3). Similarly, treatment with cyanide and salicylhydroxamic

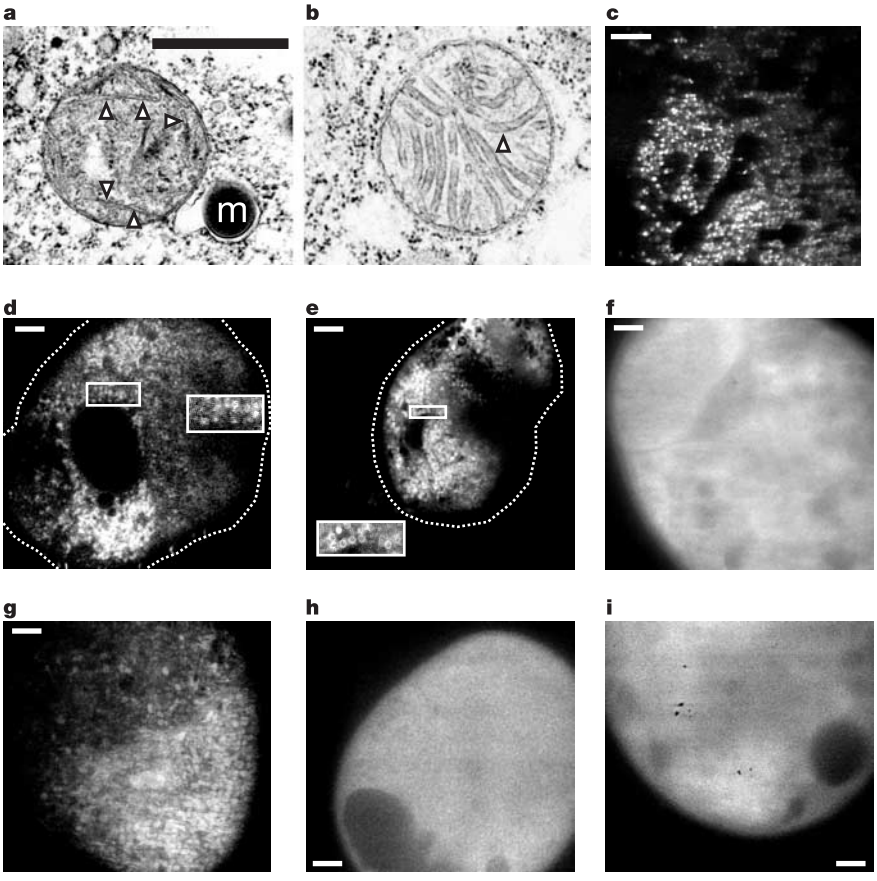

Figure 3 Hydrogenosomes of *N. ovalis* exhibit complex I activity. **a**, **b**, Electron micrographs of a hydrogenosome of *N. ovalis* (**a**) and a mitochondrion of *Euplotes* sp. (**b**). White arrowheads mark cristae; m, endosymbiotic methanogenic archaeon[15,20]. **c**, Fluorescence picture of *N. ovalis* hydrogenosomes (bright dots), which were released from the cell by gentle squashing after being stained *in vivo* with ethidium bromide. **d**, Rhodamine 123 (R123) also stains the hydrogenosomes, the only organelles matching the expected size (compare **a**, and Supplementary Information). **e**, Mitotracker green FM stains the same organelles. The inserts in **d** and **e** (outside the ciliate) show the organelles seen in the box inside the ciliate. **f**, **h**, **i**, Incubation of living cells with inhibitors of mitochondrial complex I (MPP^+ (**f**), piericidin (**h**) and rotenone (**i**))[21] completely prevents staining of the organelles by R123. **g**, Incubation with cyanide (1 mM) or antimycin A (not shown) does not interfere with staining by R123. For additional information see the text and Supplementary Information. Scale bars, 1 μm (**a**, also applies to **b**); 10 μm (**c**–**i**).

acid (SHAM), inhibitors of mitochondrial complex IV of the respiratory chain and the plant-like alternative oxidase known from certain mitochondria[3], respectively, neither killed *N. ovalis* nor interfered with its oxygen consumption under aerobic conditions (not shown). These observations not only indicate the absence of a functional complex III and IV and the absence of a terminal (plant-like) alternative oxidase, but also reveal the presence of a functional mitochondrial complex I as the source of the organellar proton gradient[3]. The oxygen consumption of *N. ovalis* observed under aerobic conditions is most probably a detoxification mechanism, and longer exposure to atmospheric oxygen kills the ciliates effectively.

Metabolic experiments using tracer amounts of uniformly labelled (U-) ^{14}C-glucose revealed that *N. ovalis* catabolizes glucose predominantly into acetate, lactate, succinate and smaller amounts of ethanol, in addition to CO_2 (Table 2). The presence of oxygen did not cause significant changes in the pattern of excreted end products (not shown). Notably, incubations in the presence of [6-^{14}C]glucose did not result in the formation of labelled CO_2. Because ^{14}C-labelled CO_2 is released from [6-^{14}C]glucose by successive decarboxylations through multiple rounds in the Krebs cycle, the absence of labelled CO_2 after application of [6-^{14}C]glucose indicates the absence of a complete Krebs cycle. The observed excretion of ^{14}C-labelled CO_2 after incubation with [U-^{14}C]glucose could be the result of either pyruvate dehydrogenase (PDH) activity, as in typical aerobic mitochondria, or pyruvate:ferredoxin oxidoreductase (PFO) activity, as in the hydrogenosomes of *T. vaginalis*. A third possibility for pyruvate catabolism, pyruvate formate lyase activity[22,23], can be excluded because no detectable amounts of formate were produced from [U-^{14}C]glucose (Table 2). We failed to identify genes for PFO but succeeded in isolating three of the four PDH genes, namely the E1α, E1β and E2 subunits, which are expressed as cDNA, indicating that *N. ovalis* uses a mitochondrial PDH for oxidative decarboxylation. Significant amounts of ^{14}C-labelled succinate from both [U-^{14}C]glucose and [6-^{14}C]glucose (Table 2) indicate that endogenously produced fumarate is used as a terminal electron acceptor, as in some anaerobic mitochondria[3]. Fumarate reduction in *N. ovalis* (to account for the production of succinate) is most probably catalysed by a membrane-bound complex II (see above; Table 1, and Supplementary Information), which is coupled to complex I through electron transport mediated by quinones[3]. Mass spectrometry coupled to liquid chromatography of lipid extracts from *N. ovalis* revealed the presence of small amounts of quinones (rhodoquinone 9 and menaquinone 8) at a concentration of about 1 pmol per mg protein (Supplementary Information). This amount is at least two orders of magnitude lower than in other eukaryotes known to possess anaerobic mitochondria producing succinate[24]. The low concentration of quinones in *N. ovalis* cells might reflect the intermediate state of their hydrogenosomes, occupying a position between mitochondria (which contain a membrane-bound electron transport chain) and previously characterized hydrogenosomes (which do not)[1,3–5,13,18].

Although an F_oF_1-ATP synthase has not yet been identified, the hydrogenosome of *N. ovalis* has retained certain basal energy-generating functions of an aerobically functioning mitochondrion[3]. To explore the presence of additional 'mitochondrial' traits in *N. ovalis*, we performed a reciprocal Smith–Waterman sequence comparison between about 2,000 six-frame-translated clones from our genomic DNA library of *N. ovalis* and the yeast[25] and human[26] mitochondrial proteins. We identified 53 additional nuclear genes encoding potential mitochondrial proteins in addition to components of the mitochondrial import machinery (Table 1, and Supplementary Information).

In contrast, the hydrogenase of *N. ovalis* does not exhibit any mitochondrial traits. This hydrogenase is rather unusual in comparison with other eukaryotic hydrogenases because it seems to be a fusion of a [Fe] hydrogenase with two accessory subunits of different evolutionary origin[4,15]. These subunits should allow NADH reoxidation in combination with the [Fe] hydrogenase, because they exhibit a significant sequence similarity to the *hox F* and *hox U* subunits of β-proteobacterial [Ni–Fe] hydrogenases, in contrast to similar, recently described hydrogenosomal proteins (24 and 51 kDa) of putative mitochondrial origin from *T. vaginalis*[18,19]. The 'mitochondrial' 24-kDa and 51-kDa genes of *N. ovalis* are clearly different from the above-mentioned hydrogenase modules and are likely to function in mitochondrial complex I (Fig. 3, Table 1, and Supplementary Information). Moreover, the catalytic centre of the hydrogenase (the H-cluster) clusters neither with any of the hydrogenases of *Trichomonas*, *Piromyces* and *Neocallimastix* studied so far, nor with any of the hydrogenase-related Nar proteins, which seem to be shared by all eukaryotes. Rather, the *N. ovalis* hydrogenase is more closely related to [Fe] hydrogenases from δ-proteobacteria[4,15,27]. These observations suggest that the hydrogenase of *N. ovalis* has been acquired by lateral gene transfer.

It should be realized that the hydrogenosome of *N. ovalis* is so far unique and not representative of all hydrogenosomes, which seem to have evolved repeatedly and independently—albeit from the same ancestral mitochondrial-type organelle. All our data identify the hydrogenosome of *N. ovalis* as a ciliate-type mitochondrion that produces hydrogen. The presence of respiratory-chain activity of mitochondrial complex I and II, in combination with hydrogen formation, characterizes the *N. ovalis* hydrogenosome as a true missing link in the evolution of mitochondria and hydrogenosomes. □

Methods

Strains

Nyctotherus ovalis ciliates were isolated from the hindgut of the cockroach *Blaberus* sp. (strain Amsterdam), taking advantage of their unique (anodic) galvanotactic swimming behaviour[28]. After the ciliate's arrival at the anode, cells were picked up with a micropipette, inspected individually under a dissecting microscope at ×40 magnification, collected in an Eppendorf tube and washed three times with anaerobic electromigration buffer. Ciliates belonging to the *Euplotes crassus/vannus/minuta* complex were cultured in artificial sea water, feeding on bacteria growing on an immersed small piece of meat (approx. 1 g of beef steak). In addition, the ciliates were fed with *Escherichia coli*, which were added at weekly intervals. Ciliates were harvested by centrifugation.

Microscopy

Electron microscopy of *N. ovalis* and *Euplotes* sp. was performed as described previously[11,15].

Fluorescence microscopy was performed with a Noran OZ video-rate confocal microscope as described previously[29]. Inhibitors were used in concentrations of 1 mM. They were dissolved in *N. ovalis* culture medium[28]. The rotenone solution contained 10% dimethyl sulphoxide, the fenazaquin solution 1% dimethyl sulphoxide.

Metabolite and quinone determinations

Micro-aerobic incubations with *N. ovalis* were performed in rotating (20 r.p.m.) sealed incubation flasks containing 5 ml incubation medium (containing 10,000–15,000 cells). All incubations were performed for 48 h and contained either 10 μCi [U-^{14}C]glucose or 10 μCi [6-^{14}C]glucose (2.07 GBq mmol^{-1}), both from Amersham. Incubations were terminated by the addition of 300 μl 6 M HCl to lower the pH from 7.2 to 2.0. *N. ovalis* cells were separated from the medium by centrifugation (5 min at 500*g* and 4 °C); excreted end products were analysed by anion-exchange chromatography on a Dowex 1X8 column. Quinones were separated by liquid chromatography and detected with a Sciex API 300 triple quadrupole mass spectrometer (see Supplementary Information).

Isolation of organellar DNA

N. ovalis cells were washed once with isolation buffer (0.35 M sucrose, 10 mM Tris-HCl pH 7, 2 mM EDTA) and disrupted in a Dounce homogenizer. Nuclei were centrifuged at 3,000*g* for 5 min, and organelles were pelleted from the supernatant at 10,000*g* for 30 min. Genomic DNA was isolated by using standard procedures or after lysis of the cells in 8 M guanidinium chloride.

Genomic DNA library

Gene-sized chromosomes were randomly amplified by PCR with telomere-specific primers, size-fractionated in agarose gels, and cloned in pGEM-T-easy (Promega). Clones with sizes between 0.5 and 5 kb were end-sequenced and analysed manually by TBLASTX (http://www.ncbi.nlm.nih.gov/BLAST). Searches were conducted with BLASTN and FASTA.

c-DNA library

RNA was isolated with the RNeasy Plant minikit (Qiagen). cDNA was prepared with the

Smart Race cDNA amplification kit (Clontech). Expressed sequence tags were amplified by PCR with the universal adapter primer provided with the kit and the various, specific internal primers.

Complete macronuclear gene-sized chromosomes

Telomere-specific primers in combination with internal gene sequences allow a straightforward recovery of the complete gene[30]. The specific (internal) primers were based on the DNA sequences of internal fragments of the various genes, which were recovered previously by PCR with degenerated primers for conserved parts of the various genes.

Phylogenetic analysis

Protein sequences were aligned with ClustalW and Muscle; unequivocally aligned positions were selected with Gblocks or manually. Phylogenies were inferred with maximum likelihood by using a discrete gamma-distribution model with four rate categories plus invariant positions and the Poisson amino acid similarity matrix, and neighbour joining as implemented in ClustalW, correcting for multiple substitutions with the Gonnet amino acids identity matrix, and bootstrapping with 100 samples.

ORFs with a lower size limit of 100 nucleotides were identified with ORF Finder (http://www.ncbi.nlm.nih.gov/gorf/gorf.html). tRNAs were identified with tRNAscan-SE (http://www.genetics.wustl.edu/eddy/tRNAscan-SE). Potential mitochondrial import signals were detected with MITOP (http://mips.gsf.de/cgi-bin/proj/medgen/mitofilter). Sequence searches were performed with BLASTX (http://www.ncbi.nlm.nih.gov/BLAST), BLASTN and FASTA. For references on phylogenetic analysis see Supplementary Information.

Received 18 August 2004; accepted 7 January 2005; doi:10.1038/nature03343.

1. Müller, M. The hydrogenosome. *J. Gen. Microbiol.* **39,** 2879–2889 (1993).
2. Roger, A. J. Reconstructing early events in eukaryotic evolution. *Am. Nat.* **154,** S146–S163 (1999).
3. Tielens, A. G. M., Rotte, C., van Hellemond, J. J. & Martin, W. Mitochondria as we don't know them. *Trends Biochem. Sci.* **27,** 564–572 (2002).
4. Embley, T. M. *et al.* Hydrogenosomes, mitochondria and early eukaryotic evolution. *IUBMB Life* **55,** 387–395 (2003).
5. Dyall, S. D., Brown, M. T. & Johnson, P. J. Ancient invasions: From endosymbionts to organelles. *Science* **304,** 253–257 (2004).
6. van der Giezen, M., Sjollema, K. A., Artz, R. R., Alkema, W. & Prins, R. A. Hydrogenosomes in the anaerobic fungus *Neocallimastix frontalis* have a double membrane but lack an associated organelle genome. *FEBS Lett.* **408,** 147–150 (1997).
7. Clemens, D. L. & Johnson, P. J. Failure to detect DNA in hydrogenosomes of *Trichomonas vaginalis* by nick translation and immunomicroscopy. *Mol. Biochem. Parasitol.* **106,** 307–313 (2000).
8. Leon-Avila, G. & Tovar, J. Mitosomes of *Entamoeba histolytica* are abundant mitochondrion-related remnant organelles that lack a detectable organellar genome. *Microbiol.* **150,** 1245–1250 (2004).
9. Fenchel, T. & Finlay, B. J. *Ecology and Evolution in Anoxic Worlds* (Oxford University Press, Oxford, UK, 1995).
10. Embley, T. M., Horner, D. A. & Hirt, R. P. Anaerobic eukaryote evolution: hydrogenosomes as biochemically modified mitochondria? *Trends Ecol. Evol.* **12,** 437–441 (1997).
11. Voncken, F. *et al.* Multiple origins of hydrogenosomes: functional and phylogenetic evidence from the ADP/ATP carrier of the anaerobic chytrid *Neocallimastix* sp. *Mol. Microbiol.* **44,** 1441–1454 (2002).
12. van der Giezen, M. *et al.* Conserved properties of hydrogenosomal and mitochondrial ADP/ATP carriers: a common origin for both organelles. *EMBO J.* **21,** 572–579 (2002).
13. Martin, W., Hoffmeister, M., Rotte, C. & Henze, K. An overview of endosymbiotic models for the origins of eukaryotes, their ATP-producing organelles (mitochondria and hydrogenosomes), and their heterotrophic lifestyle. *Biol. Chem.* **382,** 1521–1539 (2001).
14. Martin, W. & Müller, M. The hydrogen hypothesis for the first eukaryote. *Nature* **392,** 37–41 (1998).
15. Akhmanova, A. *et al.* A hydrogenosome with a genome. *Nature* **396,** 527–528 (1998).
16. Brunk, C. F., Lee, L. C., Tran, A. B. & Li, J. Complete sequence of the mitochondrial genome of *Tetrahymena thermophila* and comparative methods for identifying highly divergent genes. *Nucleic Acids Res.* **31,** 1673–1682 (2003).
17. Burger, G., Gray, M. W. & Lang, B. F. Mitochondrial genomes: anything goes. *Trends Genet.* **19,** 709–716 (2003).
18. Dyall, S. D. *et al.* Non-mitochondrial complex I proteins in a hydrogenosomal oxidoreductase complex. *Nature* **431,** 1103–1107 (2004).
19. Hrdy, I. *et al. Trichomonas* hydrogenosomes contain the NADH dehydrogenase module of mitochondrial complex I. *Nature* **432,** 618–622 (2004).
20. van Hoek, A. H. A. M. *et al.* Multiple acquisition of methanogenic archaeal symbionts by anaerobic ciliates. *Mol. Biol. Evol.* **17,** 251–258 (2000).
21. Degli Esposti, M. Inhibitors of NADH-ubiquinone reductase: an overview. *Biochim. Biophys. Acta* **1364,** 222–235 (1998).
22. Akhmanova, A. *et al.* A hydrogenosome with pyruvate formate-lyase: anaerobic chytrid fungi use an alternative route for pyruvate catabolism. *Mol. Microbiol.* **32,** 1103–1114 (1999).
23. Boxma, B. *et al.* The anaerobic chytridiomycete fungus *Piromyces* sp. E2 produces ethanol via pyruvate:formate lyase and an alcohol dehydrogenase E. *Mol. Microbiol.* **51,** 1389–1399 (2004).
24. van Hellemond, J. J., Klockiewicz, M., Gaasenbeek, C. P. H., Roos, M. H. & Tielens, A. G. M. Rhodoquinone and complex II of the electron transport chain in anaerobically functioning eukaryotes. *J. Biol. Chem.* **270,** 31065–31070 (1995).
25. Sickmann, A. *et al.* The proteome of *Saccharomyces cerevisiae* mitochondria. *Proc. Natl Acad. Sci. USA* **100,** 13207–13212 (2003).
26. Cotter, D., Guda, P., Fahy, E. & Subramaniam, S. MitoProteome: mitochondrial protein sequence database and annotation system. *Nucleic Acids Res.* **32,** D463–D467 (2004).
27. Voncken, F. G. J. *et al.* A hydrogenosomal [Fe]-hydrogenase from the anaerobic chytrid *Neocallimastix* sp L2. *Gene* **284,** 103–112 (2002).
28. van Hoek, A. H. A. M. *et al.* Voltage-dependent reversal of anodic galvanotaxis in *Nyctotherus ovalis*. *J. Eukaryotic Microbiol.* **46,** 427–433 (1999).
29. Koopman, W. J. H. *et al.* Membrane-initiated Ca^{2+} signals are reshaped during propagation to subcellular regions. *Biophys. J.* **81,** 57–65 (2001).
30. Curtis, E. A. & Landweber, L. F. Evolution of gene scrambling in ciliate micronuclear genes. *Ann. NY Acad. Sci.* **870,** 349–350 (1999).

Supplementary Information accompanies the paper on **www.nature.com/nature**.

Acknowledgements We thank L. Landweber, J. Wong and W.-J. Chang for advice on the cloning of complete minichromosomes and for sharing the first sequence of a PDH gene in *N. ovalis*; S. van Weelden and H. de Roock for help in the metabolic studies; J. Brouwers for analysis of the quinones; G. Cremers, L. de Brouwer, A. Ederveen, A. Grootemaat, M. Hachmang, S. Huver, S. Jannink, N. Jansse, R. Janssen, M. Kwantes, B. Penders, G. Schilders, R. Talens, D. van Maassen, H. van Zoggel, M. Veugelink and P. Wijnhoven for help with the isolation of various *N. ovalis* sequences; and K. Sjollema for electron microscopy. G.W.M.v.d.S., S.Y.M.-v.d.S. and G.R. were supported by the European Union 5th framework grant 'CIMES'. This work was also supported by equipment grants from ZON (Netherlands Organisation for Health Research and Development), NWO (Netherlands Organisation for Scientific Research), and the European Union 6th framework programme for research, priority 1 "Life sciences, genomics and biotechnology for health" to W.J.H.K..

Competing interests statement The authors declare that they have no competing financial interests.

Correspondence and requests for materials should be addressed to J.H.P.H. (j.hackstein@science.ru.nl). Sequences have been deposited at the EMBL database under accession numbers AF480921, AJ871267, AJ871313–AJ871361, AJ871573–AJ871576, AY608627, AY608632–AY608634, AY616150–AY616152, AY619980, AY619981, AY623917, AY623919, AY623925, AY623926, AY628683, AY628684, AY628688.

Image segmentation and lightness perception

Barton L. Anderson[1] **& Jonathan Winawer**[2]

[1]*University of New South Wales, School of Psychology, Sydney, New South Wales 2052, Australia*
[2]*Massachusetts Institute of Technology, Brain and Cognitive Sciences, Cambridge, Massachusetts 02139, USA*

The perception of surface albedo (lightness) is one of the most basic aspects of visual awareness. It is well known that the apparent lightness of a target depends on the context in which it is embedded[1–6], but there is extensive debate about the computations and representations underlying perceived lightness. One view asserts that the visual system explicitly separates surface reflectance from the prevailing illumination and atmospheric conditions in which it is embedded[7–10], generating layered image representations. Some recent theory has challenged this view and asserted that the human visual system derives surface lightness without explicitly segmenting images into multiple layers[11,12]. Here we present new lightness illusions—the largest reported to date—that unequivocally demonstrate the effect that layered image representations can have in lightness perception. We show that the computations that underlie the decomposition of luminance into multiple layers under conditions of transparency can induce dramatic lightness illusions, causing identical texture patches to appear either black or white. These results indicate that mechanisms involved in decomposing images into layered representations can play a decisive role in the perception of surface lightness.

The amount of light projected to the eyes (luminance) is determined by a number of factors: the illumination that strikes visible surfaces, the proportion of light reflected from the surface and the amount of light absorbed, reflected or deflected by the prevailing atmospheric conditions (such as haze or other partially transparent media). Only one of these factors, the proportion of light reflected (lightness), is associated with an intrinsic property of